DOI: http://dx.doi.org/10.12989/scs.2003.3.2.111

Shear-lag effect in twin-girder composite decks

Luigino Dezi†, Fabrizio Gara‡, and Graziano Leoni‡

Institute of Structural Engineering, University of Ancona, via Brecce Bianche, 60131, Ancona, Italy

(Received July 15, 2002, Accepted March 12, 2003)

Abstract. The paper presents a model for analysing the shear-lag effect on the slab of twin-girder composite decks subjected to static actions, support settlements and concrete shrinkage, which are the main actions of interest in composite bridge design. The proposed model includes concrete creep behaviour and shear connection flexibility. The shear-lag in the slab is accounted for by means of a new warping function. The considered actions are then applied to a realistic bridge deck and their effects are discussed. The proposed method is utilised to determine the slab effective widths for three different width-length ratios of the deck. Finally, a comparison between the results obtained with the Eurocode EC4-2 and those obtained with the proposed model is performed.

Key words: composite steel-concrete bridges; effective width; flexible shear connection; long term behaviour; shear-lag effect.

1. Introduction

Steel-concrete composite continuous decks are widely used in viaducts and bridges with medium span length (40-100 m). Such decks are usually composed of two steel beams, even in the case of wide concrete slabs (>20 m), that can be sustained by cantilevered cross-beams or be transversally prestressed (Fig. 1). As is well known, in this kind of structure the usual assumption of bending theory, according to which the plane cross-sections remain plane after loading, is not realistic. The slab undergoes significant warping (Von Kármán 1924), which induces a non-uniform stress distribution on the slab cross-section, also known as shear-lag effect. Since this effect depends on the beam-slab interface shear-flow, a refined model should take account of the shear connection flexibility, which permits slip at the slab-beam interface and increases the global flexibility of the structure. Furthermore, concrete creep behaviour, which produces a redistribution in time of the internal forces between slab and steel beam modifying the stress distribution on the slab, should be included.

In practical applications, these aspects are usually considered separately by means of simplified methods suggested by the technical codes (EC4-2 1997). The non-uniform stress distribution on the slab is evaluated by reducing the slab width (effective width method), while a modified Young's modulus is introduced to take into account the concrete creep. Simplified rules are also employed to evaluate the local effects on the connection produced by longitudinal concentrated forces or by the concrete shrinkage and thermal action on the slab. Furthermore, it is important to underline that the

†Professor and Head of Institute
‡Research Assistant

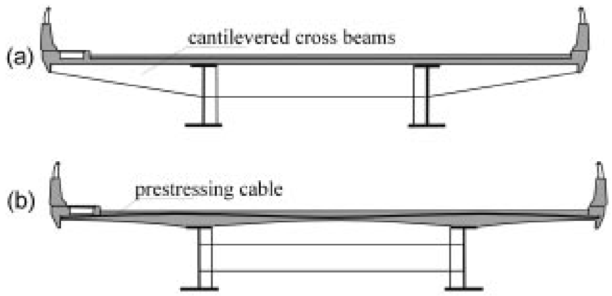

Fig. 1 Twin-girder composite decks: (a) with cantilevered cross-beams; (b) with transversally prestressed slab

formulae suggested by technical codes for the effective slab width were obtained and validated for external static actions (Sedlacek and Bild 1993); their use for other kinds of actions, such as geometrical actions (support settlements), concrete shrinkage and thermal actions, is not supported either by numerical analyses nor by experimental tests.

In this paper, a method for time-dependent analysis of shear-lag effect in twin-girder composite decks, also taking into account the shear connection deformability, is presented.

A model recently developed by the authors for single steel-concrete composite beams (Dezi *et al*. 2001), is generalised to analyse twin-girder decks for any steel beam spacing, by introducing a suitable warping function in order to describe the shear-lag effect on the slab. The main actions of interest in bridge design, namely static actions, geometrical actions (settlement of support) and concrete shrinkage are considered separately in order to evaluate the effective slab width and its variation in time for each different action. The numerical solution is obtained by introducing a double discretization, along the time domain and the beam axis, and by using the step-by-step procedures and the finite differences method. With reference to a realistic bridge deck some numerical applications are carried out considering each action separately; the results obtained are then compared with those given by the method of the effective width suggested by the Eurocode EC4-2.

2. Model description

The typical steel-concrete composite twin-girder deck of Fig. 2 is considered. The external loads are positioned so as to avoid torsion, distortion, and transverse bending of the deck cross-section. In order to take into account the flexibility of the shear connection and the shear-lag effect of the slab, the classical Newmark model (Newmark *et al*. 1951), which assumes the preservation of the plane cross-section for concrete slab and steel beam considered separately, is modified according to the Reissner hypothesis (Reissner 1946), for which the slab loss of planarity due to shear-lag is described by the product between a fixed warping shape of the cross-section (warping function) and a scalar function defining the warping intensity along the beam axis (shear-lag function).

The shear-lag analysis in twin-girder decks should take into account the actual position of the beams [Fig. 2(a)].

The problem can be solved by introducing two shear-lag functions, the first for the slab cantilevers and the second for the internal section, as shown in Dezi and Mentrasti (1985). Alternatively, only one shear-lag function may be used in conjunction with a more complex function which describes warping

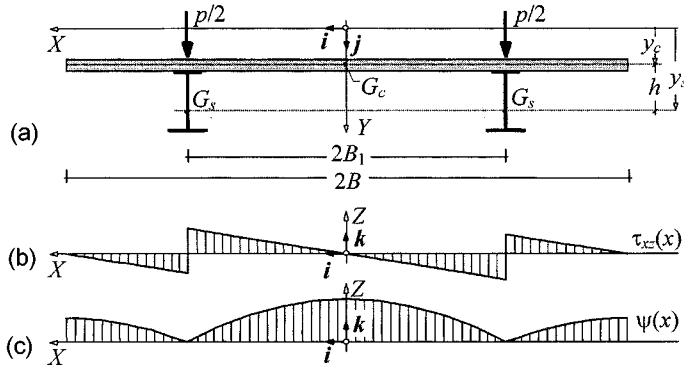

Fig. 2 (a) Composite twin-girder deck; (b) shear stress distribution; (c) warping function

throughout the slab width. This paper proposes a unique warping function with two different branches [Fig. 2(c)].

By adopting the reference frame and the notations of Fig. 2, the displacement field, at a generic instant t, is then expressed by the following equations:

$$\boldsymbol{u}(x, y, z; t) = v(z; t)\boldsymbol{j} + [w_c(z; t) - (y - y_c)v'(z; t) + f(z; t)\psi(x)]\boldsymbol{k} \quad \text{for the concrete slab} \tag{1}$$

$$\boldsymbol{u}(x, y, z; t) = v(z; t)\boldsymbol{j} + [w_s(z; t) - (y - y_s)v'(z; t)]\boldsymbol{k} \quad \text{for the steel beam} \tag{2}$$

in which v denotes the vertical displacement of the composite cross-section, w_c and w_s are the axial displacements of the concrete slab and the steel beam, respectively, and f is the function which measures the intensity of the slab warping described by the shape function ψ constant on the slab thickness (Dezi *et al.* 2001). From Eqs. (1) and (2), the following expression of the interface slip can be easily derived:

$$\Gamma(z; t) = w_s(z; t) - w_c(z; t) + hv'(z; t) \tag{3}$$

Furthermore, as a result of Eqs. (1) and (2), the steel beam is subjected only to axial strain while both axial and shear strains are present in the concrete slab.

The analysis is performed under the hypothesis of linear elastic behaviour for the steel beam and shear connection, which is assumed to be spread along the beam length.

The concrete is a viscoelastic material affected by axial and shear strain components; the following two integral-type constitutive relationships are thus introduced:

$$\sigma_z(x, y, z; t) = \int_{t_0}^{t} R_E(t, \vartheta)d[\varepsilon_z(x, y, z; \vartheta) - \bar{\varepsilon}(\vartheta)] \tag{4}$$

$$\tau_{xz}(x, y, z; t) = \int_{t_0}^{t} R_G(t, \vartheta)d\gamma_{xz}(x, y, z; \vartheta) \tag{5}$$

where $R_E(t, \vartheta)$ and $R_G(t, \vartheta)$ are the axial and shear relaxation functions, namely the stress components at time t due to the relevant unit strain components (ε_z and γ_{xz}) applied at time ϑ and maintained constant in time; $\bar{\varepsilon}$ is an imposed strain representing the concrete shrinkage or the thermal strain.

Both these relationships are also considered for concrete under tensile stresses, which is supposed to be uncracked.

The shear relaxation function is derived by means of the following equation:

$$R_G(t, \vartheta) = \frac{1}{2(1+\upsilon)} R_E(t, \vartheta) \tag{6}$$

which considers the concrete Poisson ratio υ constant in time. This approximation is usually accepted in literature (Chiorino *et al.* 1984) although experimental data regarding the variation in time of Poisson ratio are not available.

By assuming as unknowns the displacements previously defined (v, w_c, w_s and f), the following solving system is derived (Dezi *et al.* 2001):

$$-\rho(w_s - w_c + v'h) - \int_{t_0}^{t} R_E(t, \vartheta) d[A_c(w_c'' - \bar{\varepsilon}') + S_\psi f''] = 0 \tag{7}$$

$$\rho(w_s - w_c + v'h) - E_s A_s w_s'' = 0 \tag{8}$$

$$-h\rho(w_s' - w_c' + v''h) + E_s I_s v'''' + \int_{t_0}^{t} R_E(t, \vartheta) I_c dv'''' = p \tag{9}$$

$$\int_{t_0}^{t} R_E(t, \vartheta) d\left[-S_\psi(w_c'' - \bar{\varepsilon}') - I_\psi f'' + \frac{I_{d\psi} f}{2(1+\upsilon)}\right] = 0 \tag{10}$$

where p is the vertical load; A_c, A_s and I_c, I_s are the areas and the moment of inertia of the concrete slab and steel beam cross-section, respectively, E_s is the Young's modulus of the steel beam, ρ is the stiffness per unit length of the shear connection and

$$S_\psi = \int_{A_c} \psi da, \qquad I_\psi = \int_{A_c} \psi^2 da, \qquad I_{d\psi} = \int_{A_c} \psi_{,x}^2 da \tag{11a,b,c}$$

are the cross-sectional properties related to the slab loss of planarity. From a physical point of view, Eqs. (7) and (8) translate the axial equilibrium condition of the concrete slab and the steel beam, respectively; Eq. (9) translates the vertical equilibrium condition of the composite element and Eq. (10) is an overall equilibrium condition between shear and axial stresses in the concrete slab.

The problem solution is obtained by completing the solving system with the relevant boundary conditions. As is well known, they express the kinematical effects of external restraints or, in the case of free boundary, the dual static conditions. For the sake of simplicity in Table 1 the most common boundary conditions are reported. In particular, in the case of geometrical actions, the solving Eqs. (7)-(10) are homogeneous and the support settlement $\bar{v}$ is imposed in the fourth kinematical condition. Similarly, even in the case of uniform shrinkage or thermal action, the solving system is homogeneous and the relevant strains $\bar{\varepsilon}$ are imposed in the first and in the last static conditions.

2.1. Warping function

As previously stated, the shear-lag analysis of twin-girder decks should take into account the actual

Table 1 Boundary conditions

Kinematical conditions	Static conditions
$w_c = 0$	$\int_{t_0}^{t} R_E(t, \vartheta) d[A_c(w_c' - \bar{\varepsilon}) + S_\psi f'] = 0$
$w_s = 0$	$E_s A_s w_s' = 0$
$v' = 0$	$-\int_{t_0}^{t} R_E(t, \vartheta) I_c dv'' - E_s I_s v'' = 0$
$v = \bar{v}$	$-\int_{t_0}^{t} R_E(t, \vartheta) I_c dv''' - E_s I_s v''' + h\rho(w_s - w_c + v'h) = 0$
$f = 0$	$\int_{t_0}^{t} R_E(t, \vartheta) d[S_\psi(w_c' - \bar{\varepsilon}) + I_\psi f'] = 0$

position of the beams. In fact, even if the deck is symmetric, it cannot be divided into two symmetric beams [Fig. 2(a)] and the usual warping functions available in literature are not suitable. For this reason a new warping function describing the non-uniform stress distribution on the whole slab width is introduced.

As a consequence of the small thickness of the slab, the warping function may be assumed to be constant on the slab thickness, so that $\psi(x, y) \cong \psi(x)$. The warping function can be derived from the local equilibrium condition of the slab considered as a thin walled beam (Laudiero and Savoia 1990). Under the assumption of zero body forces and by neglecting the shear stress component τ_{yz}, the stress τ_{xz} on the middle plane of the slab [Fig. 2(b)] can be obtained by integrating the following equilibrium equation:

$$\frac{\partial \tau_{xz}}{\partial x} + \frac{\partial \sigma_z}{\partial z} = 0 \tag{12}$$

By assuming, at a first level of approximation, σ_z as uniformly distributed on the slab width, the local longitudinal equilibrium condition for the concrete slab provides

$$\frac{\partial \sigma_z}{\partial z} = \frac{q}{A_c} \tag{13}$$

where q is the global longitudinal shear flow due to the slab beam interaction. Thus, the following expressions for τ_{xz} are obtained:

$$\tau_{xz}(x, z) = \frac{q(z)}{A_c}(x + B) \qquad -B \le x \le -B_1 \tag{14a}$$

$$\tau_{xz}(x, z) = \frac{q(z)}{A_c}x \qquad -B_1 < x \le +B_1 \tag{14b}$$

$$\tau_{xz}(x, z) = \frac{q(z)}{A_c}(x - B) \qquad +B_1 < x \le +B \tag{14c}$$

where B and B_1 are clearly defined in Fig. 2.

By denoting with G the shear modulus of elasticity, the usual stress-strain elastic relationship holds

$$u_{z,x} + u_{x,z} = \frac{1}{G}\tau_{xz}(x, z) \tag{15}$$

By assuming that u_x (horizontal transverse displacement) is zero on the whole slab, u_z can be obtained by integrating Eq. (15) with respect to x. By taking into account expressions (14), the longitudinal displacements can be expressed as

$$u_z = \frac{q(z)B^2}{2A_cG}\psi(x) + c(z) \tag{16}$$

where

$$\psi(x) = \left(\frac{x}{B}\right)^2 + 2\frac{x}{B} + \frac{B_1}{B}\left(2 - \frac{B_1}{B}\right) \qquad -B \le x \le -B_1 \tag{17a}$$

$$\psi(x) = \left(\frac{x}{B}\right)^2 - \left(\frac{B_1}{B}\right)^2 \qquad -B_1 < x \le +B_1 \tag{17b}$$

$$\psi(x) = \left(\frac{x}{B}\right)^2 - 2\frac{x}{B} + \frac{B_1}{B}\left(2 - \frac{B_1}{B}\right) \qquad +B_1 < x \le +B \tag{17c}$$

is a warping function which is zero at the beam-slab joints.

The warping function obtained is thus constituted by three parabolic branches: in the general case the external branches are different from the internal branch [Fig. 2(c)] while, in the simple case in which $B_1 = B/2$, the warping function components (17) assume the same maximum value both at the middle and at the edges of the slab.

3. Numerical solution

Eqs. (7)-(10) constitute a coupled integral-differential system in which the four functions v, w_c, w_s and f are the problem unknowns. The system cannot be solved in closed form and thus a numerical solution has to be calculated.

The first problem encountered in the numerical solution deals with the calculation of the relaxation function. In fact, the main creep models are expressed in terms of creep functions; given the complexity of these expressions, the relevant relaxation functions must be numerically evaluated by integrating a Volterra's integral equation (Chiorino *et al*. 1984). In order to avoid the preliminary onerous calculations providing the relaxation function, the problem can be switched to a dual form enforcing the relationship holding between the creep and relaxation problems

$$f(t) = \int_{t_0}^{t} R_E(t, \vartheta)\, dg(\vartheta) \Leftrightarrow g(t) = \int_{t_0}^{t} J(t, \vartheta)\, df(\vartheta) \tag{18}$$

This leads to a different coupled system of integral-differential equations in which only the creep function J is involved

$$-[A_c(w_c'' - \varepsilon_{cs}') + S_\psi f''] - \rho \int_{t_0}^{t} J(t, \vartheta) d(w_s - w_c + v'h) = 0 \tag{19}$$

$$-E_s A_s w_s'' + \rho(w_s - w_c + v'h) = 0 \tag{20}$$

$$I_c v'''' + \int_{t_0}^{t} J(t, \vartheta) d[E_s I_s v'''' - h\rho(w_s' - w_c' + v''h)] = \int_{t_0}^{t} J(t, \vartheta) dp \tag{21}$$

$$-S_\psi(w_c'' - \varepsilon_{cs}') - I_\psi f'' + \frac{I_{d\psi} f}{2(1+\upsilon)} = 0 \tag{22}$$

The numerical solution of this problem requires the discretization both of the time domain and the beam axis. The first is necessary to transform the time integrals appearing in the system into an algebraic form by applying the trapezoidal integration rule. The second permits solving the differential system by means of the finite difference method. In this way the solution of the integral-differential problem is obtained by a step-by-step procedure by solving a sequence of linear algebraic problems.

For the details of the numerical procedure readers can refer to Dezi *et al.* (2001).

4. Shear-lag analysis for different actions

In this section, the results of elastic and time-dependent analyses of a two-span composite bridge deck, with the cross-section shown in Fig. 3, are reported. It is assumed that the presence of cantilevered cross-beams, required to support the thin slab, does not affect the longitudinal deck behaviour. Three different actions are considered separately: static action constituted by a uniformly distributed load, geometrical action constituted by settlement of the middle support and a uniform concrete volume reduction due to concrete shrinkage. As is well known, the results obtained in the last case can be extended to the case of uniform thermal action in the slab.

The effective slab width (B_{eff}) is here calculated by means of the well known formula (Von Kármán 1924):

$$B_{eff} = B\frac{\int_{A_c} \sigma_z da}{A_c \sigma_{\max}} \tag{23}$$

where σ_z is the normal stress in the concrete.

The creep and shrinkage functions suggested by the CEB-FIP model code 1990 (1988) are considered

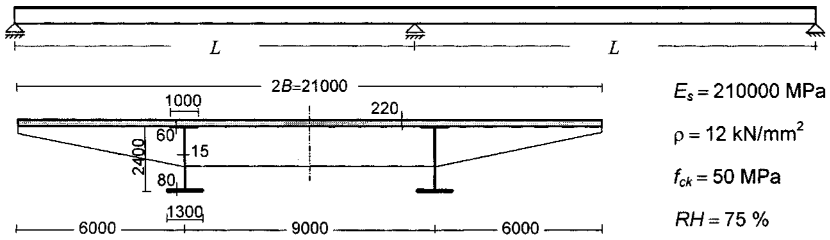

Fig. 3 Static scheme and cross-section of the deck

by assuming the concrete strength $f_{ck} = 50$ MPa and the relative humidity $RH = 75\%$. The initial time of the analysis is $t_0 = 28$ days in the cases of static load and support settlement while the concrete shrinkage begins at casting time; the final time of the analysis is $t = 20000$ days.

It has been observed that bridge decks possess high values of shear connection stiffness and that their range of variation is very limited. It has also been reported in Gara *et al*. (2001) that the results of the analysis are not affected by varying the values of the shear connection stiffness in this particular range. For this reason a typical shear connection stiffness (ρ) has been utilised in the following discussion.

The concrete is considered to be uncracked even in the tension regions of the slab. This simplifying assumption is meaningful only when the slab is prestressed. However the problem linearity permits the superposition of effects produced by different actions and the results reported here evidence the shear-lag effect for each action considered separately.

4.1. Static action (uniformly distributed load)

The normal stresses produced in the concrete slab by two uniformly distributed loads applied along the axes of the steel beams are illustrated in Fig. 4. The longitudinal distributions of the normal stress calculated at mid-height of the concrete element along the edge of the slab and above the steel beams are illustrated in Fig. 4(a). These are calculated for both the initial and final time. In Fig. 4(b) the transverse distributions of the normal stresses in the slab at two cross-sections are shown, one located along the beam (cross-section 1) and one located at inner support (cross-section 2).

As it is well known, the shear-lag effect strongly modifies the transverse stress distribution at the cross-section over the internal support, while it is less important on the span.

The effective slab width B_{eff} is also shown by dashed lines in Fig. 4(b). For cross-section 1, B_{eff} is about 94% of the geometrical width, while for cross-section 2 it reduces to 72%. It is important to note that the effective width is practically constant in time, both in the span and at the middle support.

4.2. Geometrical action (support settlement)

Fig. 5 outlines the results obtained by imposing a settlement to the middle support. As in the previous

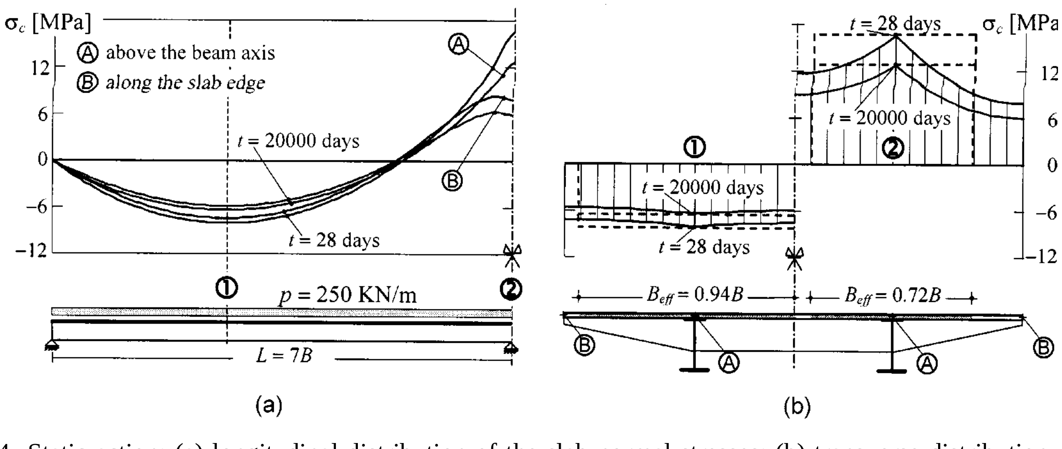

Fig. 4 Static action: (a) longitudinal distribution of the slab normal stresses; (b) transverse distribution of the slab normal stresses

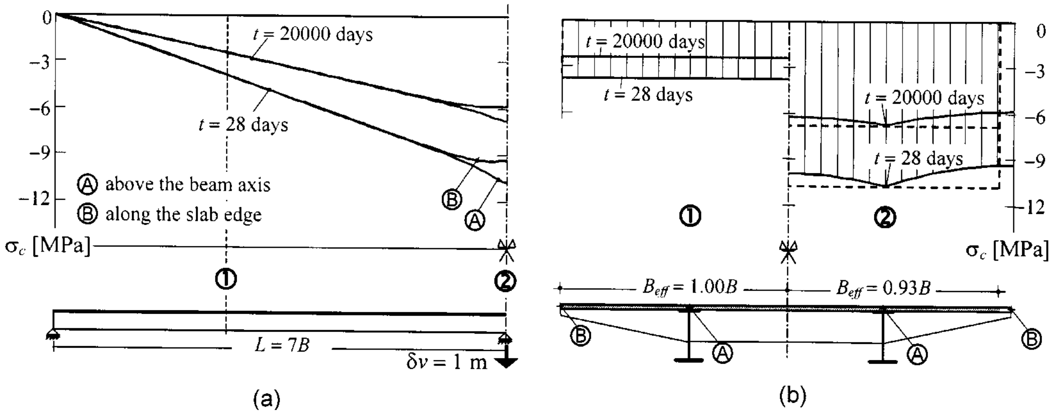

Fig. 5 Geometrical action: (a) longitudinal distribution of the slab normal stresses; (b) transverse distribution of the slab normal stresses

loading case, the longitudinal distributions of the normal stresses calculated along the slab edge and above the steel beam are shown in Fig. 5(a), while their transverse distribution calculated at two cross-sections are shown in Fig. 5(b).

In this case, the shear-lag effect appears to be significant only near the internal support for a length approximately equal to half the deck width, while at other cross-sections along the beam length the transverse distributions of the normal stresses remain uniform. At the middle support, the effective width is about 93% of the geometrical slab width. Even in this case the effective slab width is fairly constant in time.

By comparing the results obtained for static and geometrical actions, very significant differences in the effective slab width may be observed. Consequently, in practical applications, when support settlements are imposed to introduce longitudinal slab prestressing, two different effective slab widths should be introduced to evaluate the normal stresses produced by the two kinds of action.

4.3. Concrete shrinkage

Fig. 6 shows the results produced by the drying shrinkage of concrete slab at 90 days after concrete casting and at the final time of the analysis. The longitudinal distributions of the normal stresses along the slab edge are reported in Fig. 6(a), while the transverse distributions at cross-sections near the external support (cross-section 0) and at the middle support (cross-section 2) are shown in Fig. 6(b). The stresses are calculated at mid-height of the concrete slab for the final time of the analysis.

At locations along the beam length other than those near the external supports, the distribution of the normal stresses due to shrinkage is similar to that produced by a settlement of the internal supports. The effective slab width is practically coincident with the geometrical width in the span and reduces to 96% at the middle support cross-section.

The regions at the ends of the beam are characterised by a significant shear-lag effect, due to the longitudinal shear force distribution at the beam-slab interface, even if the stress state in the slab is less important. The diagram of Fig. 6(a) (dashed line) shows the interface shear force distribution along the beam axis at the final time of the analysis which assumes the maximum value at the beam end.

The conclusions drawn for the concrete shrinkage can be also extended to the case of a uniform

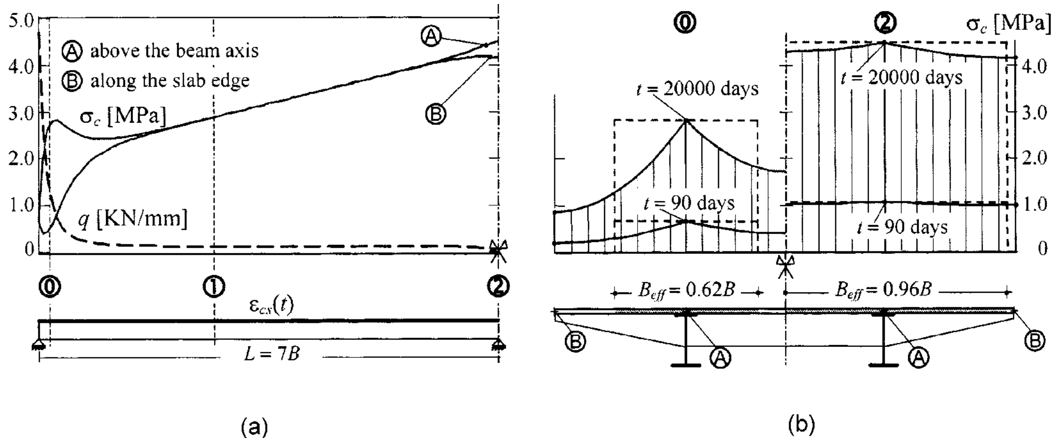

Fig. 6 Concrete slab shrinkage: (a) longitudinal distribution of the slab normal stresses and shear flow at beam-slab interface; (b) transverse distribution of the slab normal stresses

thermal action on the slab. In both cases the slab is affected by an imposed uniform strain distribution which induces a similar stress field.

4.4. Influence of the width-length ratio

The effective widths are calculated for each action separately and for three different deck width-length ratios. The stresses obtained with these analyses are then compared with those obtained using the EC4-2 (1997).

As previously shown, concrete creep does not significantly modify the effective width in time. Fig. 7 shows the time evolution of the effective width of cross-sections 1 and 2 for each action considered. For this reason only the elastic results of the applications considered are illustrated in the following figures.

Fig. 8(a) highlights the dependence of shear-lag effect on the width-length ratio and on the loading conditions. The shear-lag effect is more important for the static action than for support settlement and concrete shrinkage (or uniform thermal action on the slab), both in the span and near the middle support. In the case of static action, the effective slab width is not reported in the section included between the dashed lines, because in this region the stress resultant is almost zero and the effective width is not significant.

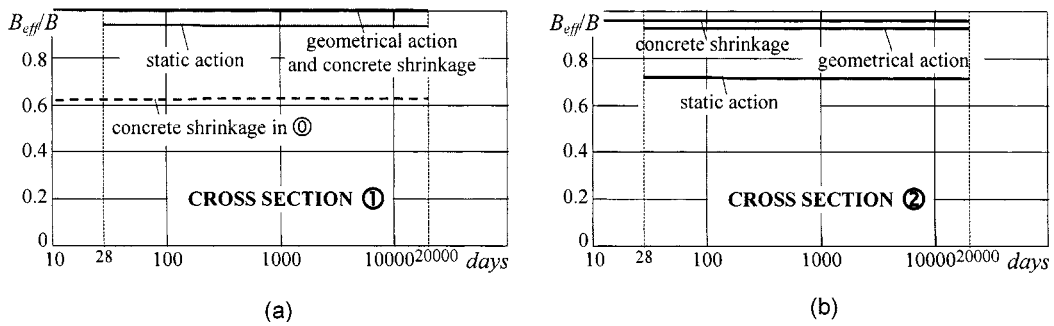

Fig. 7 Time evolution of effective width: (a) cross-section 1; (b) cross-section 2

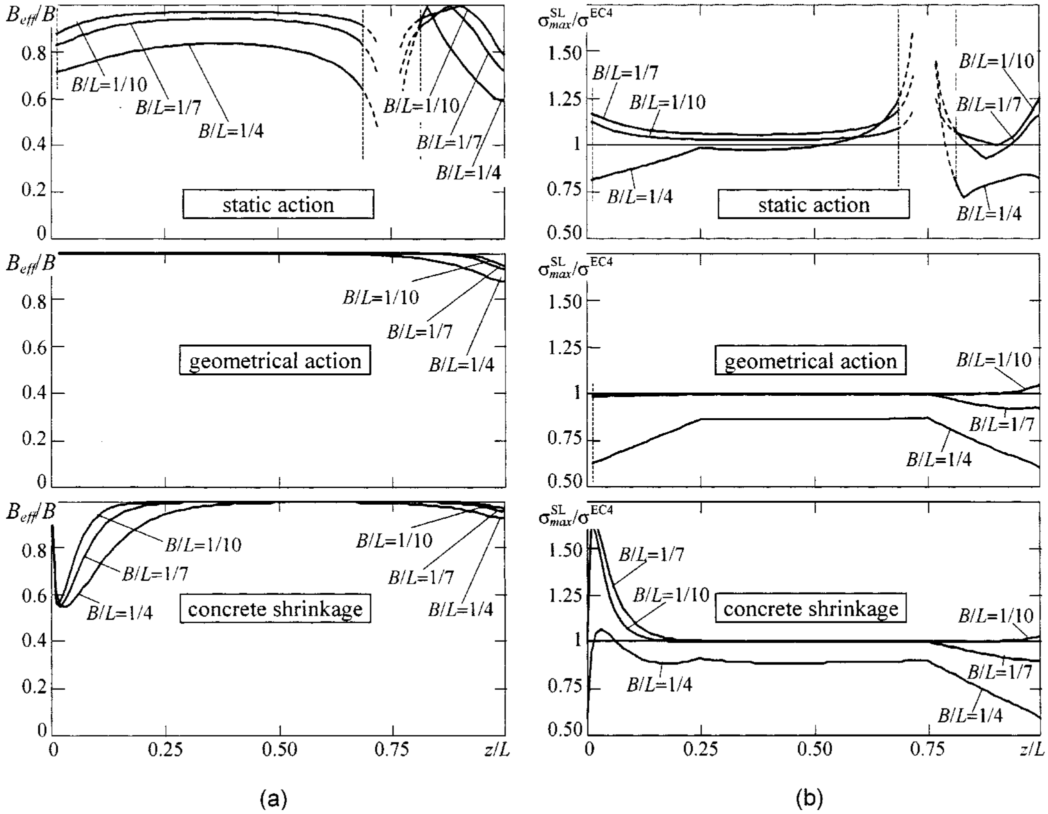

Fig. 8 (a) Effective width given by the model presented; (b) comparison with EC4-2

Fig. 8(b) shows a comparison between the results obtained with the method presented and the one recommended by EC4-2; the curves represent the ratios between the maximum value of the normal stresses calculated with the model presented and the value obtained by the method suggested by the EC4-2. In the case of static actions, differences of about ±20% are observed for the extreme cases of short (B/L = 1/4) and long (B/L = 1/10) spans. For geometrical actions and concrete shrinkage, larger differences (about 40%) are observed for wide decks.

This result is particularly important for geometrical actions, such as settlement of supports, which are usually imposed to induce slab prestressing. In this case, in fact, the effective width suggested by the EC4-2 overestimates the stress state produced by the support settlement and consequently leads to a non conservative solution. This aspect is important in practical applications and should be investigated in more detail even in the case of composite decks prestressed by means of both internal and external cables.

5. Conclusions

In this paper, the shear-lag effect in twin-girder composite decks has been investigated by means of an analytical model taking into account the shear connection flexibility and concrete creep. A new warping function, which describes the non-uniform stress distribution on the whole slab width considering the actual position of the beams, was introduced. The main actions of interest in bridge design, such as static actions, settlement of supports, and concrete shrinkage, were considered. The normal stress distributions and the effective slab widths were evaluated both at initial and at final time and then compared with those calculated in accordance with EC4-2. The following conclusions may be drawn:

- in all the actions considered, the shear-lag effect is not substantially modified by concrete creep and consequently the effective slab width can be considered as constant in time;
- the shear-lag effect is more important for static actions than for support settlements, concrete shrinkage and uniform thermal action on the slab;
- the effective widths suggested by technical codes give better solutions for static actions than for support settlements or shrinkage. Their use for geometrical actions leads to an overestimation of the maximum values of the normal stress in the slab. This result assumes a certain importance in practical applications, where support settlements are imposed in order to prestress the concrete slab and the code results are not conservative.

References

CEB-FIP model code 1990 (1988), *C.E.B. Bullettin d'Information n. 190*, C.E.B. - F.I.P. Comité Euro-International du Beton, Paris.

Chiorino, M.A., Napoli, P., Mola, F. and Koprna, M. (1984), *C.E.B. design manual on structural effects on time-dependent behaviour of concrete*, *C.E.B. Bullettin d'Information n. 142/142bis*, Georgi Publishing Co., Saint-Saphorin, Switzerland.

Dezi, L., Gara, F., Leoni, G., and Tarantino, A. M. (2001), "Time-dependent analysis of shear-lag effect in composite beams", *J. Mech. Engrg.*, ASCE, **127**(1), 71-79.

Dezi, L., and Mentrasti, L. (1985), "Nonuniform bending-stress distribution (Shear-lag)", *J. Struct. Engrg.*, ASCE, **111**(12), 2675-2690.

EC4-2 (1997), *EUROCODE 4: Design of composite steel and concrete structures - Part 2: Bridges*, European Committee for Standardization.

Gara, F., Leoni, G., and Tarantino, A. M. (2001), "Mutual effects between creep, connection deformability and shear-lag in steel-concrete composite bridges", *Proceedings of Concreep-6*, 20-22 August 2001, M.I.T. Cambridge, USA, 785-790.

Laudiero, F., and Savoia, M. (1990), "Shear strain effects in flexure and torsion of thin-walled beams with open or closed cross-section", *Thin Walled Structures,* **10**, 87-119.

Newmark, N. M., Siess, C. P., and Viest, I. M. (1951), "Test and analysis of composite beams with incomplete interaction", *Proc. Soc. Exp. Stress Anal.*, **9**(1), 75-92.

Reissner, E. (1946), "Analysis of shear-lag in box beams by the principle of the minimum potential energy", *Quarterly of Appl. Math.*, **4**(3), 268-278.

Sedlacek, G., and Bild, S. (1993), "A simplified method for the determination of the effective width due to shear lag effects", *J. Construct. Steel Research*, **24**, 155-182.

Von Kármán, Th. (1924), "Beitrag zur technischen mechanik und technischen physik", *A. Föppl-Festschroft*, 114-127.

CC